Available online at www.sciencedirect.com
SCIENCE DIRECT®
Optics Communications 247 (2005) 171–180
OPTICS COMMUNICATIONS
www.elsevier.com/locate/optcom

Range of plasma filaments created in air by a multi-terawatt femtosecond laser

G. Méchain [a,*], C.D'Amico [a], Y.-B. André [a], S. Tzortzakis [a,1], M. Franco [a], B. Prade [a], A. Mysyrowicz [a], A. Couairon [b], E. Salmon [c], R. Sauerbrey [d]

[a] *Laboratoire d'Optique Appliquée, Centre National de la Recherche, Unité Mixte de Recherche 7639, Ecole Nationale Supérieure de Techniques Avancées – Ecole Polytechnique, Chemin de la Hunière, F-91761 Palaiseau Cedex, France and Teramobile project*
[b] *Centre de Physique Théorique, Ecole Polytechnique, CNRS UMR 7644, Palaiseau 91128, France*
[c] *Laboratoire de spectrométrie ionique et moléculaire, CNRS UMR 5579, Université Lyon I, 69622 Villeurbanne, France and Teramobile project*
[d] *Institut fur Optik und Quantenelektronik, Jena, 07743, Germany and Teramobile project*

Received 8 July 2004; received in revised form 9 November 2004; accepted 11 November 2004

Abstract

The propagation of a multi-terawatt femtosecond laser pulse in air is studied as a function of initial chirp. The chirp conditions for optimising air ionisation at long distance are presented. Ionisation channels are observed over a distance reaching 400 m.

PACS: 42.25.Bs; 42.65.Re; 42.65.Jx; 52.38.Hb; 52.35.Mw
Keywords: Femtosecond filamentation; Ultrashort laser pulses

1. Introduction

There is increasing interest in the study of femtosecond laser self-guiding (filamentation) in air and other transparent media. The physical processes underlying this effect are now well understood. Filamentation arises predominantly from a dynamic competition between the optical Kerr effect, which leads to beam self-focusing and air ionisation by multi-photon absorption, preventing beam collapse by beam defocusing [1,2]. Air ionisation involves the simultaneous absorption of at least 8 infrared photons, so that it occurs for a threshold like intensity $I \sim 10^{13}$ W/cm^2. In the case of an input power close to the critical power for

* Corresponding author. Tel.: +33 1693 19702; fax: +33 1693 19996.
E-mail addresses: mechain@enstay.ensta.fr (G. Méchain), stzortz@greco2.polytechnique.fr (S. Tzortzakis).
[1] Present address: Laboratoire d'Utilisation des Lasers Intenses, UMR 7605, CNRS-CEA-Universite Paris VI- Ecole Polytechnique, 91128 Palaiseau, France.

0030-4018/$ - see front matter © 2004 Elsevier B.V. All rights reserved.
doi:10.1016/j.optcom.2004.11.052

filamentation ($P_{cr} \approx 5$ GW for air at normal pressure and a laser central wavelength of 800 nm), the main features of the filament which is formed, such as spectral broadening, pulse shortening, beam contraction and plasma channel formation, are in good agreement with numerical simulations that solve a non linear Schrödinger equation for the envelope of the propagating field [3–6]. At higher input power, $P \gg P_{cr}$, the beam splits into a large number N of filaments, with $N \approx P/P_{cr}$ [7–9]. This situation is less well understood, due on the one hand to the complexity of numerical simulations which require a full "3d + 1" treatment over a long path [5,10,30] and on the other hand to the difficulty in measuring the beam characteristics over long propagation distances $D > 100$ m, due to the sensitivity of the multifilamentary pattern on the initial beam characteristics and on atmospheric turbulence.

Long-range filamentation of femtosecond laser pulses in air can lead to several applications [11]. The broad white continuum generated during self-guided propagation can be exploited for multi-component LIDAR studies of air pollution [12–14]. The creation of plasma column can be used to trigger and guide electric discharge, and eventually can lead to a new type of lightning rod [15–17]. Finally, the high local intensity of the self-guided laser pulse can be used for laser-induced plasma spectroscopy (LIPS) of remote targets [18]. Thus, depending on the particular application, it is important to maximise either continuum generation, the length of ionisation channels or the laser intensity at long distance.

One important laser parameter in this respect is the initial chirp of the laser pulse. For ultra-short pulses at 800 nm, the pulse duration is expected to increase because of group velocity dispersion of air. This detrimental effect can be precompensated by imparting a negative initial chirp [19,20]. Initial chirped laser pulse has another effect. By increasing the pulse duration at constant pulse energy, it decreases its peak power [21]. This is expected to increase the distance necessary for the onset of filamentation [23] and also to reduce the number N of generated filaments.

In this paper, we report experimental results concerning the long propagation of IR multi-terawatt laser pulses on a horizontal path. Measurements are performed as a function of initial laser chirp. We are particularly interested in measuring the length over which ionised plasma channels are formed. We also investigate the conditions for optimal continuum generation at long distance $D > 600$ m.

2. Experimental procedure

The experiments have been performed with a Ti:Sapphire multi-terawatt laser system, called Teramobile. A detailed description of the laser is given in [21]. The laser operates with a central wavelength at 800 nm and an energy per pulse of up to 190 mJ at a repetition rate of 10 Hz. The beam diameter at the output of the compressor is 34 mm with a pronounced top-hat profile, as shown in Fig. 1. Since the laser is based on the chirped pulse amplification (CPA) technique [24,25], the initial chirp of the laser pulse can be easily adjusted. For the present campaign, the laser final compression stage was modified so that it could produce pulses with a negative chirp (shorter wavelength first) varying between 0.2 and 9.6 ps pulses. This corresponds to respectively 190 and 4 times the critical value $P_{cr} = 5$ GW for

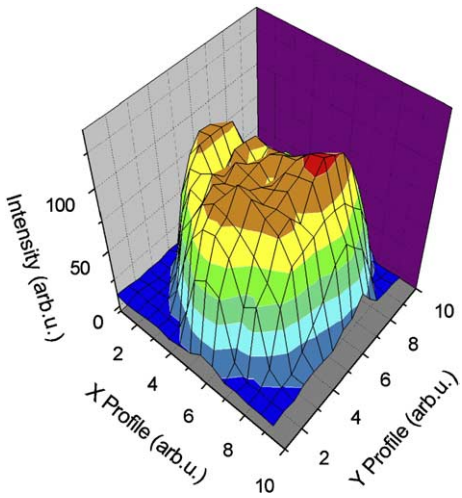

Fig. 1. Profile of the beam. Intensity recorded at the output of the compressor.

laser pulses at 800 nm. This implies that the initial power of the laser is always higher than the critical power necessary to create filaments in air. In order to obtain large negative chirps, one of the gratings of the compressor was mounted on a 40-mm translation stage. The compressor was calibrated with an autocorrelator measuring the pulse duration as a function of the distance between the gratings, yielding the value 241 fs/mm. The collimated laser beam was launched horizontally 3 m above a paved road to a maximum distance of 600 m. Longer distances of 1000 and 2350 m were also available.

Measurement of the beam intensity in a filament is a difficult task, even in the case of a well-controlled single filament in the laboratory. The most reliable method, which is based on the generation by a filament of high order odd harmonics in an atomic gas cell [26], requires an elaborate set-up with precise alignment. Additional difficulties in the present case are the high input power, leading to multifilamentary structures that may vary from shot to shot, and the effect of air turbulence [29], which produces fluctuations in the position of the beam at long distance.

In view of these difficulties, we have adopted the following procedure. We first measure the occurrence of air ionisation as a function of distance for a given initial laser chirp. Optical field ionisation of air is detected with two electric techniques described below. The onset of ionisation yields a precise value of the laser intensity, which is independently known both from experiments in single filament and from simulations. Next we correlate the ionisation signal measured as a function of distance with the darkening of preexposed photographic paper (Kodak linagraph paper, type 1895). To confirm this calibration, the same procedure is repeated in the laboratory using a well-characterized single filament. This procedure allows us to determine in a single shot the intensity profile in a complex multifilamentary pattern at a given distance with an order-of-magnitude accuracy.

Calibration of the photographic paper in the laboratory proceeds as follows. First, we measure the electric conduction of the plasma channel using the method described in [27]. Two electrodes with small holes in their centre and separated by 3 cm are placed in the filament path. A potential difference of 1000 V is applied between the electrodes. The conducting channel formed by the filament between the electrodes closes the electric circuit and induces a current that is monitored across a load resistance of 8.2 kΩ. Keeping constant the interelectrode distance and moving the circuit along the propagation axis, one obtains a characteristic ionisation curve as shown in Fig. 2(b) (black squares). A second technique measures directly the electric signal obtained when the filament impinges on the exposed copper tip of a coaxial cable connected to an oscilloscope [28]. This induces a voltage measured with a low inductance electric circuit (grey triangles).

Both types of signals recorded as a function of distance, are shown in Fig. 2(b). For comparison, we also show in Fig. 2(c) the calculated length of the plasma channel and the corresponding laser intensity in the filament for the same experimental conditions. These results have been obtained by solving numerically the non-linear Schrödinger equation governing the slowly varying envelope of the laser field [6]. Various physical effects are taken into account: diffraction, group velocity dispersion and higher-order dispersive terms, self-focusing, stimulated Raman scattering, plasma absorption and defocusing, space-time focusing and self-steepening. More details on the physical model used in the code can be found in [6]. Since the results in Fig. 2 correspond to single filaments produced in laboratory experiment, 2 + 1 dimensional simulations were performed by assuming revolution symmetry around the propagation axis. Usually, a resolution of 10 microns in the transverse direction and 1–3 fs in the time direction is sufficient but much higher resolution can be achieved with fixed step size or with adaptative mesh if necessary. As can be seen in Fig. 2(c), there is a sharp threshold-like onset of ionisation when the laser intensity reaches the value 10^{13} W/cm^2; this correspond to an electric signal of 10–30 mV induced in the coaxial cable. For the same points in the path of the filament, pictures of the beam profile were also recorded on a photosensitive paper in single shot exposures. The black spot recorded on the photographic paper was scanned

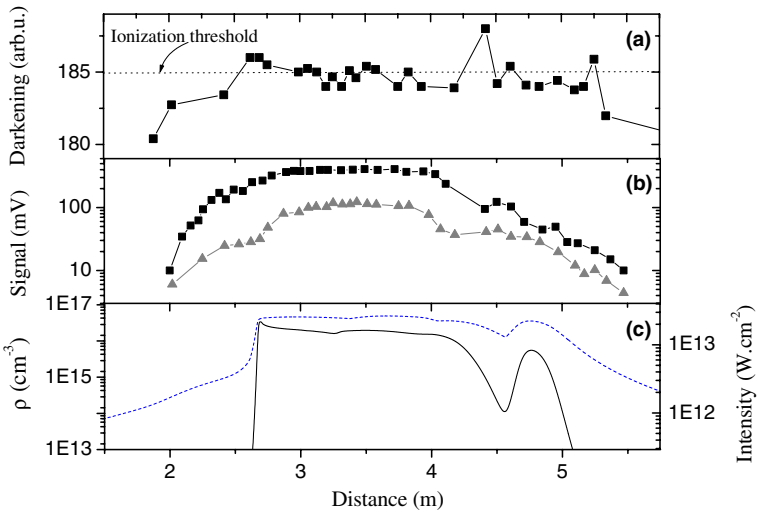

Fig. 2. (a) Darkening of a photographic papers measured along the laser propagation axis. (b) Electric conductivity of air (black square) and induced voltage on a coaxial detector (grey triangle) measured along the laser propagation axis. (c) Numerical simulation. The black continuous line represents the electron density (ρ) (scale on the left axis). The dotted line gives the intensity in the core of the filament (scale on the right axis).

and its darkening was plotted as a function of propagation distance. The value of darkening corresponding to the ionisation threshold is given at the extremities of the plasma string at $z = 2.6$ and at $z = 5.1$ m. This corresponds to a value around 185 (in arbitrary units) for the darkening curve of the photographic paper (see Fig. 2(a)). It is adopted as the minimum value for which ionisation of air occurs in long-range propagation experiments. In this range of value the photographic paper is in a saturated regime.

The same procedure relating electric and photographic exposure traces has been applied to outdoor, long distance experiments for two different laser chirps. First, the electric conductivity of the plasma channel was measured for a pulse duration stretched to 0.2 ps. For this chirp value, the observed filaments are rather reproducible in position from shot to shot and can be tracked over several tens of meters of propagation. Measurements recorded at several points along the propagation are reported in Fig. 3(a). To assess the darkening of the photographic papers that corresponds to the ionisation threshold, the last value of the plateau on the electric signal has been related to the degree of darkening at the same distance. The deduced value is about 185 in arbitrary units, consistent with the value obtained in the laboratory experiment.

We have also measured the electric signal for an initial pulse stretched to 2.4 ps. In this case, fluctuations in position become more important, making the electric conductivity measurement unreliable. We have instead recorded the electric signal produced by the central wire of the coaxial cable placed on the beam (see Fig. 3(b)). As discussed above, the ionisation threshold is reached for an electric signal of about 10 mV. This corresponds to a darkening of about 188 in arbitrary units, as shown in Fig. 3, in accordance with the previous results. We have therefore used the darkening of the paper as method to characterize the multi-filamentary-pattern, for various initial chirps on the beam path.

3. Long-range beam characterisation

One series of photographic exposures recorded at four distances, 21, 50, 68, and 109 m is shown in Fig. 4 for a negative initial pulse duration of 1.2 ps. One can clearly observe in the transverse

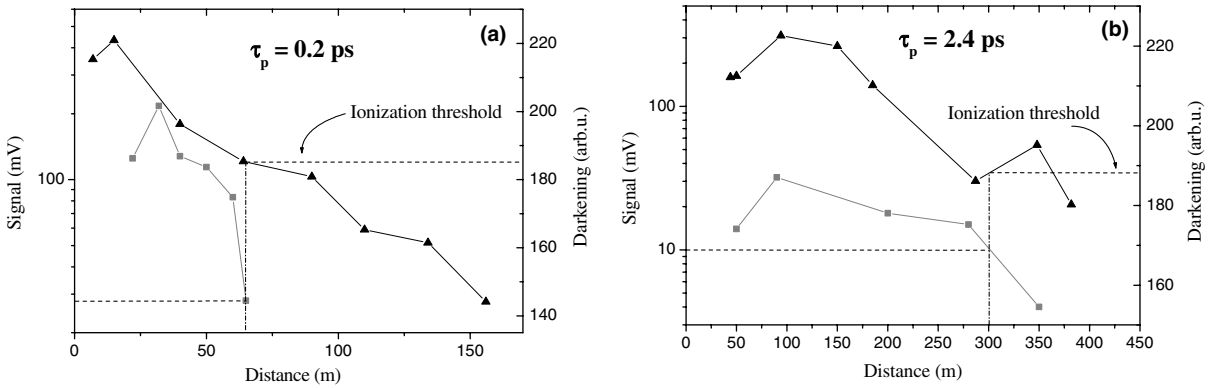

Fig. 3. (a) Comparison of the darkening between photosensitive paper (black triangle) and electric conductivity measurements (grey square) for a pulse duration stretched to 0.2 ps. (b) Comparison between photosensitive paper (black triangle) and coaxial cable measurements (grey square) for a pulse duration stretched to 2.4 ps.

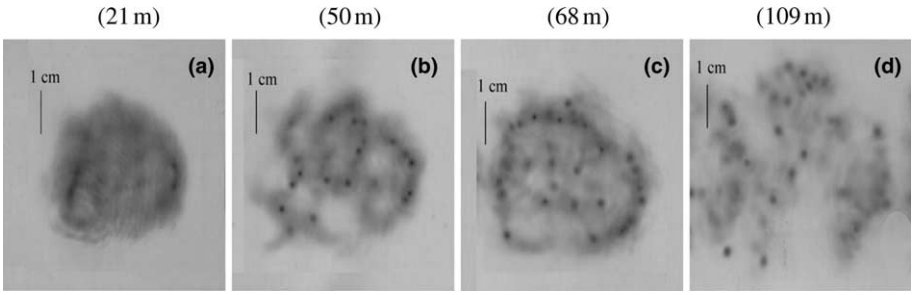

Fig. 4. Measured beam profile at various distances with a initial pulse duration stretched to 1.2 ps.

section of Fig. 4(a)–(c) the appearance of a number of high intensity channels that tend to appear on a ring at the periphery of the beam. This highly uneven intensity distribution of the beam intensity profile persists after a hundred meters of propagation (Fig. 4(d)). High intensity channels are also linked by an energy web organization. The ring like multi-filamentary structure can be understood, by considering the initial superGaussian beam profile (see Fig. 1). Since the self-focusing process initiates filamentation by excitation of a limited range of transverse wavenumbers [7], one expects few filaments in the centre of the beam, because of its flat intensity profile corresponding to wavenumbers having a weak amplification rate, and an accumulation of filaments around the beam edge, where intensity gradients are maximum. As shown in Fig. 5, this behaviour is well reproduced numerically by the same three-dimensional + time propagation code used in [10,30]. The physical model is that described in [30] and takes account of the afore mentioned effects. The code follows a split step Crank–Nicholson, Fourier (in time) scheme. Unevenly distributed adaptative mesh grids allow us to adjust the resolution to the wide range of spatial and temporal scales. The initial beam intensity profile at $d = 0$ (see Fig. 1) is introduced in the code as an initial condition. 10^5 spatial grid points in the transverse dimension were sufficient to reproduce the light tubes shown in Fig. 5(a) with a resolution of 100 μm. The temporal resolution was varied in the range 3–15 fs. No atmospheric turbulence is included in these calculations, first because the patterns recorded experimentally were rather reproducible from shot to shot, second because the scale of viscous dissipation is about 1 mm [29] which is slightly larger that the light tubes and third because it is mainly the intensity

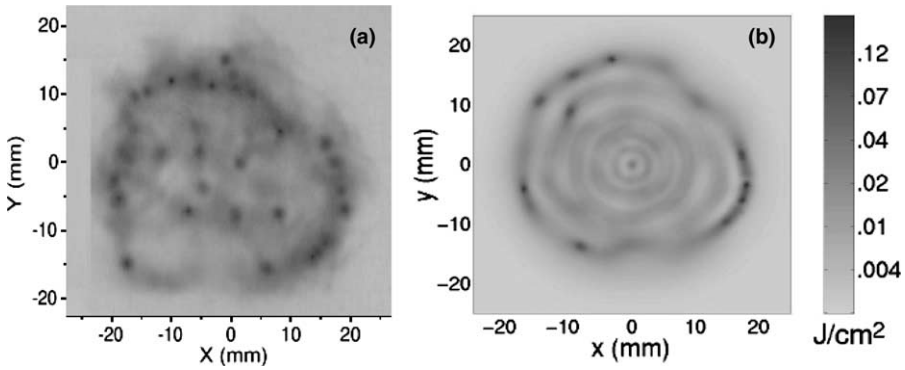

Fig. 5. Comparison between experiment and simulation after 68 m of propagation for a beam initially stretched to 1.2 ps. (a) Beam cross-section recorded with a photosensitive paper. (b) Computed distribution of fluence.

gradients in the nearly top hat beam profile (see Fig. 1) which are responsible of the organization of the light channels on the periphery of the input beam. A much cleaner beam with regular azimuthal perturbations was numerically shown to produce similar patterns except that the light tubes are regularly located on polygonal figures [30].

The photographic papers have been scanned in a densitometer through the highest intensity spots. Results are shown in (Fig. 6). Between $d = 50$ and 68 m, the trace is saturated or even burned (Fig. 6(a)). At longer distances, one observes a broadening of the spot size and a decrease of the darkening. From such measurements, one deduces that air ionisation takes place over a distance of up to 100 m.

In Fig. 7, a count of the number of hot spots giving a signal exceeding the ionisation threshold and a count of the number of light channels are given for three representative chirps as a function of distance. Light channels are defined here to be high intensity spots within the beam profile with insufficient intensity to ionise air. The intensity of light channels is in the range 5×10^{10}–10^{13} W/cm^2 as deduced from the darkening of photographic plates comprised between 145 and 185

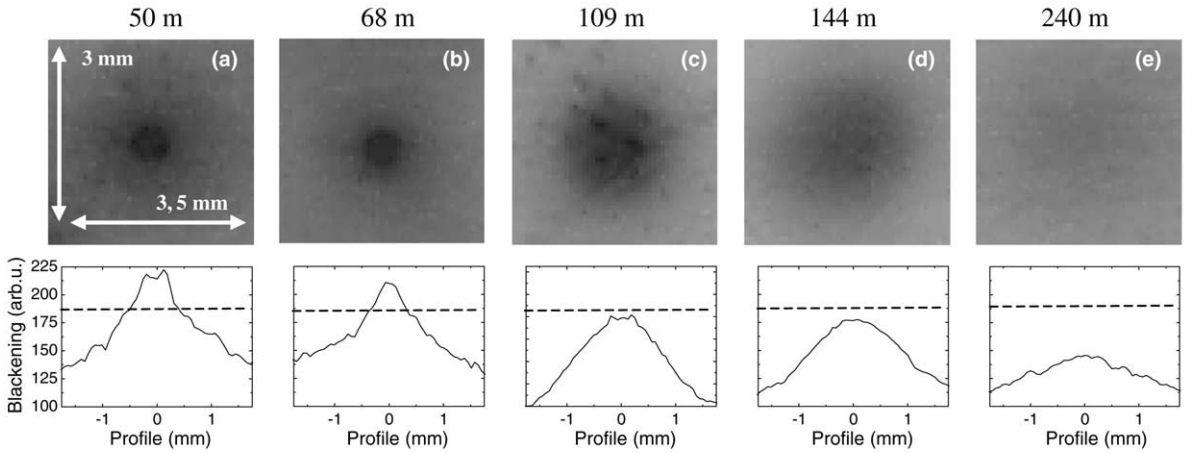

Fig. 6. Experimental burning spots of the laser on photographic paper at five various distances and for an initial pulse duration of $\tau_p = 1.2$ ps. For each distance, the intensity profile has been reported below, dotted lines show the ionisation threshold (in arbitraries units).

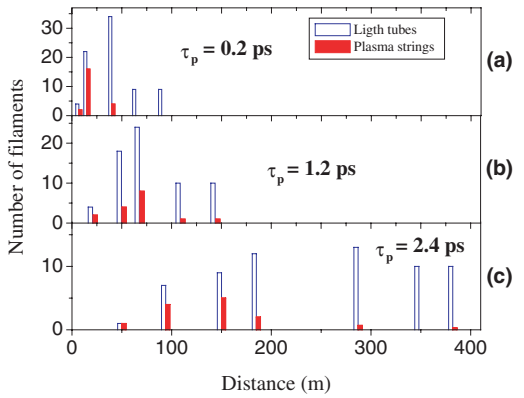

Fig. 7. Evolution of the number of filaments in step with distance for three consecutive pulse duration: (a) 0.2 ps, (b) 1.2 ps, (c) 2.4 ps.

(see Fig. 11(c)). Adopting the criterion that an ionising filament is formed if, at least one hot spot has a peak intensity exceeding the threshold value for ionisation (darkening >185, see Fig. 6), one can draw the filament length as a function of laser chirp. It is plotted in Fig. 8 as black lines. When the initial pulse duration is increased by introducing a negative chirp the peak power decreases. Filamentation occurs later but over a longer distance and with less plasma strings. For the pulse duration τ_p = 2.4 ps the length where ionisation occurs has been increased by more than a factor of 5 and

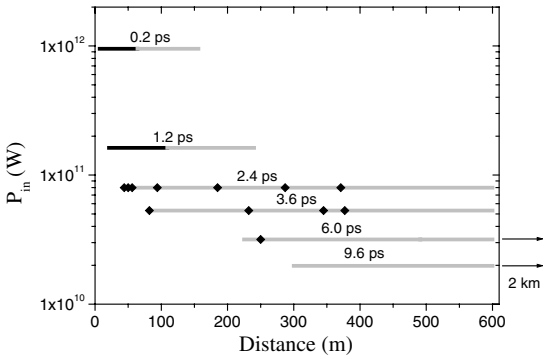

Fig. 8. Evolution of the length of filamentation by varying the initial chirp of the laser pulse. The pulse without chirp has a duration of 100 fs. The black lines and black points refer to locations where air ionisation could be detected, grey lines to distances where bright light channels are observed.

the number of filaments has been divided by 3. In a recent work, Golubtsov et al. [22] reported numerical simulations on the control of filamentation and the generation of supercontinuum by also varying the initial pulse-phase modulation (PPM). They predicted that a negative PPM shift the beginning of filamentation [16,21–23,31] and significantly extend the length of plasma channels. With an initial pulse duration of 800 fs and a negative PPM, the filamentation length reaches 800 m and is 2.5 times longer than with the transform-limited pulse (τ_0 = 21 fs). Our results are qualitatively comparable to most of the predictions made from the calculations of Golubtsov et al. [22]. Nevertheless, the calculated length of plasma channels is much longer than our experimental optimum. The numerical ionisation length reaches 800 m with a pulse duration of 800 fs, even though we find a maximum length of 300 m for a pulse duration of 2.4 ps. Numerical results sensitively depends on the specific shape of the input beam, the initial pulse parameters and experimental results depend also on the dynamics of plasma detection. This explains discrepancies between their simulations and our experiments, despite clear common general trends. Finally, the grey lines in Fig. 8 correspond to the formation of intense light channels, without occurrence of detectable ionisation. As reported recently, such bright light channels without measurable ionisation propagate over at least 2350 m [10].

The procedure using photosensitive paper has been repeated for various initial pulse duration with the results summarized in Fig. 9. The degree of darkening of papers corresponding each time to the strongest spots within the entire beam profile has been traced as a function of distance for different initial negative chirps. In the same figure, the value of the ionisation threshold is plotted as a horizontal dashed line. The degree of darkening for each curve above the ionisation value should be considered with circumspection, because the paper becomes saturated or even burned. However, it gives a rather reliable criterion for the onset of ionisation and therefore allows us to extract the distance over which air is ionised. An optimum was found for a negatively chirped pulse (duration of 2.4 ps). For this value, ionisation was observed

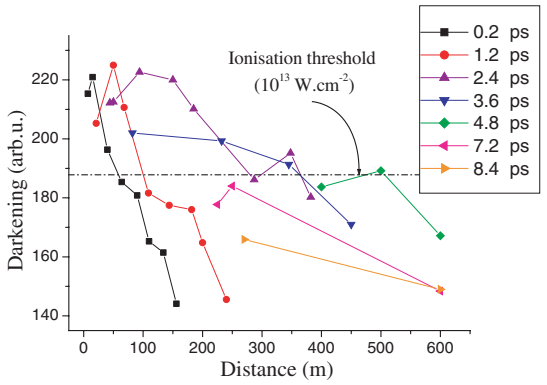

Fig. 9. Measurement of maximum of intensity in light filament as a function of distance for various stretched pulse durations.

over more than 300 m with a maximum of five ionising filaments in the beam profile.

Finally, we briefly address the question of optimising white continuum generation at long distance. The beam intercepted by a white screen was photographed with a digital camera at several distances. In Fig. 10, the beam cross-section recorded at 1000 m is compared for two values of the chirp, 0.2 and 9.6 ps. The first corresponds to the smallest duration of the pulse that can be realized with the modified compressor stage, the second gives the highest negative chirp achievable. One notices in the first case a bright continuum generation, without discernible hot spots, with a beam divergence of 1 mrad. In the second case, the whole beam profile is slightly compressed, and bright channels (which persists beyond 2350 m) are clearly observable.

For the longest pulse duration, 9.6 ps, photographs of the beam profile recorded at a distance of 2350 m are shown in Fig. 11(a) and (b). As discussed earlier, we were not able to measure reliable evidence of air ionisation under these conditions. An estimate of the laser intensity from the darkening of the photographic paper gives a peak value of about 10^{12} W/cm^2.

Assuming a conversion efficiency of 1–10% between the initial pulse and the broadband continuum, we can now estimate the total power as well as the fluence of the continuum on a distance of 1 km, since we know the white continuum beam divergence. We find an energy of 2–20 mJ in a continuum comprise between 300 and 950 nm and a fluence of 2×10^{-7}–2×10^{-6} J/cm^2 for an initial pulse duration close to minimum. On the other, with a negative chirp giving a pulse duration of 9.6 ps, we have typically between 5 and 7 light channels at 1 km. Only the bright channels generate continuum in this case. Assuming the same conversion efficiency into continuum of 1–10%, the continuum energy is in the ratio of (total surface of light tubes/beam surface) $\sim10^{-6}$. However, the fluence is the same. Therefore, we conclude that a small negative chirp is better suited for applications where the continuum emission must be maximized.

The fact that ionisation is usually needed for balancing self-focusing is a physical picture that emerged from works on filaments generated by unchirped pulses at moderate powers. With multiple filaments generated by high-power beams, this picture is expected to be still correct for indepen-

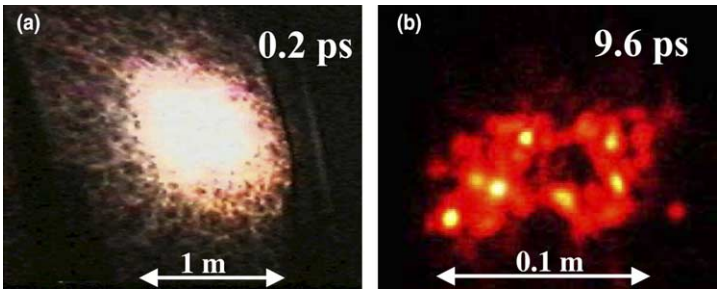

Fig. 10. Comparison between two beam cross-section at 1000 m. (a) minimum negative chirp: 0.2 ps, (b) maximum negative chirp: 9.6 ps.

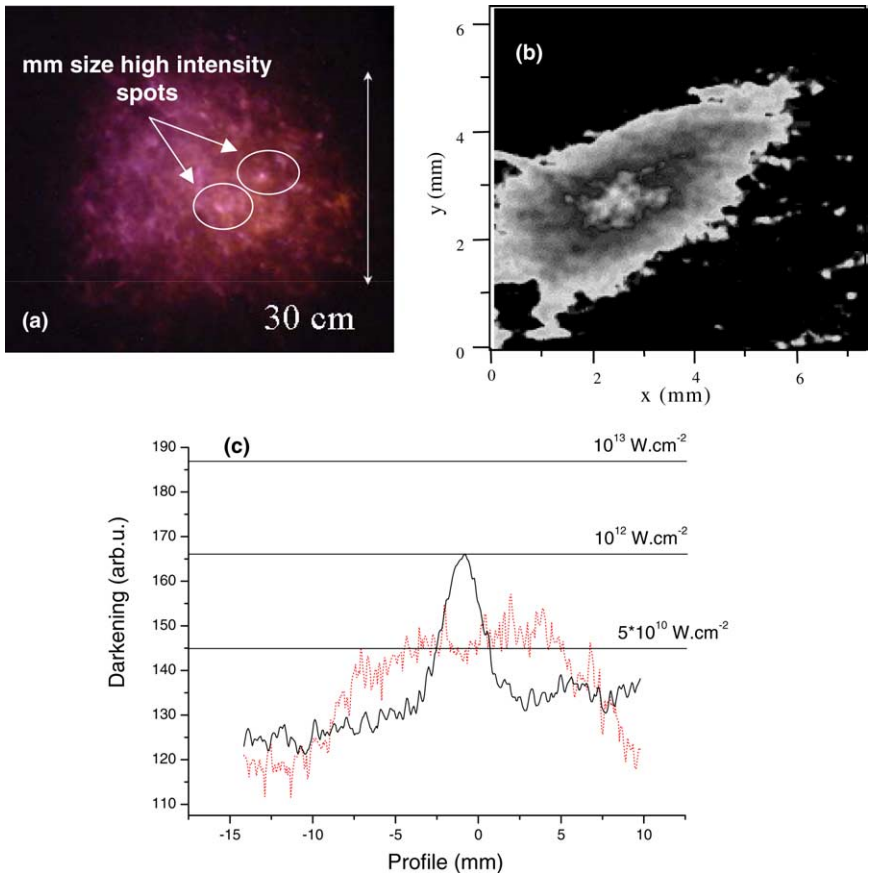

Fig. 11. Experiment at 2350 m. The beam had initial chirp of 9.6 ps. (a) Photography of the beam cross-section intercepted by a white screen. Exposure time of a few second. (b) Detail of a single shot light tube recorded with photosensitive paper. (c) Transverse profile (continuous curve) of the light tube at 2350 m. The dash curve represents the measured curve in laboratory (energy $E = 20$ mJ, pulse duration 130 fs, diameter $\Phi = 2$ cm) to determine the lower intensity limit of the light tubes.

dent filaments collapsing on themselves, a situation favoured with unchirped pulses. With powerful beams and large chirps, a large number of light tubes compete for the available laser energy over extended distance. The validity of this powerful concept of the energy reservoir, originally proposed in [5], was shown in detail for a single filament [32]. The collapse of a specific light channel into a plasma filament is more difficult when surrounding light channels prevent a fast concentration of power, which makes other mechanism such as, e.g., GVD, more efficient to arrest the collapse before ionisation occurs [33].

In conclusion, we have studied the beam profile of an intense IR femtosecond laser pulse as a function of distance, up to 2350 m, for different initial chirps. Using electric measurements and photographic recordings, we estimated the distance over which air ionisation was occurring. A maximum ionisation distance of 370 m was found for a laser with a negative chirp of 2.4 ps. A shorter pulse duration favoured the amount of broadband continuum detected at long distance, while longer negative chirps led to the appearance of bright light channels at 2350 m, the longest distance for which measurements were performed. The peak

intensities of such bright light spots was estimated to be around 10^{12} W/cm^2.

Acknowledgements

This work has been funded by a special CNRS-DFG program, called Teramobile. A.M. is grateful to the Humboldt foundation for support.

References

[1] A. Braun, G. Korn, X. Liu, D. Du, J. Squier, G. Mourou, Opt. Lett. 20 (1995) 73.
[2] E.T.J. Nibbering, P.F. Curley, G. Grillon, B.S. Prade, M.A. Franco, F. Salin, A. Mysyrowicz, Opt. Lett. 21 (1996) 62.
[3] O.G. Kosareva, V.P. Kandidov, A. Brodeur, C.Y. Chien, S.L. Chin, Opt. Lett. 22 (1997) 1332.
[4] M. Mlejnek, E.M. Wright, J.V. Moloney, Opt. Lett. 23 (1998) 382.
[5] M. Mlejnek, M. Kolesik, E.M. Wright, J.V. Moloney, Phys. Rev. Lett. 83 (15) (1999) 2938.
[6] A. Couairon, G. Méchain, S. Tzortzakis, M. Franco, B. Lamouroux, B. Prade, A. Mysyrowicz, Opt. Commun. 225 (2003) 177.
[7] V.I. Bespalov, V.I. Talanov, JETP Lett. 3 (1966) 307.
[8] B. LaFontaine, F. Vidal, Z. Jiang, C.Y. Chien, D. Comtois, A. Desparois, T.W. Johnson, J.-C. Kieffer et, H. Pépin, Phys. Plasmas 6 (1999) 1615.
[9] Miguel Rodriguez, Riad Bourayou, Guillaume Méjean, Jérôme Kasparian, Jin Yu, Estelle Salmon, Alexander Scholz, Bringfried Stecklum, Jochen Eislöffel, Uwe Laux, Artie P. Hatzes, Roland Sauerbrey, Ludger Wöste, Jean-Pierre Wolf, PRE 69 (2004) 036607.
[10] G. Méchain, A. Couairon, Y.-B. André, C. D'Amico, M. Franco, B. Prade, S. Tzortzakis, A. Mysyrowicz, R. Sauerbrey, Appl. Phys. B 79 (2004) 379.
[11] J. Kasparian, M. Rodriguez, G. Méjean, J. Yu, E. Salmon, H. Wille, R. Bourayou, S. Frey, Y.-B. André, A. Mysyrowicz, R. Sauerbrey, J.-P. Wolf, L. Wöste, Science 301 (2003) 61.
[12] L. Wöste, C. Wedekind, H. Wille, P. Rairoux, B. Stein, S. Nikolov, Ch. Werner, St. Niedermeier, F. Ronneberger, H. Schillinger, R. Sauerbrey, Laser Optoelektron. 29 (1997) 51.
[13] J. Yu, D. Mondelain, G. Ange, B. Volk, S. Niedermeier, J.P. Wolf, J. Kasparian, R. Sauerbrey, Opt. Lett. 26 (2001) 533.
[14] G. Méjean, J. Kasparian, J. Yu, S. Frey, E. Salmon, J.-P. Wolf, Appl. Phys. B 78 (2004) 535.
[15] X.M. Zhao, J.-C. Diels, C.Y. Wang, J.M. Elizondo, IEEE J. Quantum Electron. 31 (1995) 599.
[16] M. Rodriguez, R. Sauerbrey, H. Wille, L. Wöste, T. Fujii, Y.–B. André, A. Mysyrowicz, L. Klingbeil, K. Rethmeier, W. Kalkner, J. Kasparian, E. Salmon, J. Yu, J.-P. Wolf, Opt. Lett. 27 (2002) 772.
[17] D. Comptois, et al., IEEE Trans. Plasmas Sci. 31 (2003) 377.
[18] Ph. Rohwetter, J. Yu, G. Méjean, K. Stelmaszczyk, E. Salmon, J. Kasparian, J.-P. Wolf, L. Wöste, J. Anal. Atom Spectrom. 19 (2004) 437.
[19] G. Yang, Y. Shen, Opt. Lett. 9 (1984) 510.
[20] A.L. Gaeta, Phys. Rev. Lett. 84 (2000) 3582.
[21] H. Wille, M. Rodriguez, J. Kasparian, D. Mondelain, J. Yu, A. Mysyrowicz, R. Sauerbrey, J.-P. Wolf, L. Wöste, Eur. Phys. J. AP 20 (2002) 183.
[22] I.S. Golubtsov, V.P. Kandidov, O.G. Kosareva, Quantum Electron. 33 (2003) 525.
[23] J.H. Marburger, Prog. Quantum Electron. 4 (1975) 35.
[24] D. Steickland, G. Mourou, Opt. Commun. 56 (1985) 219.
[25] P. Maine, D. Strickland, P. Bado, M. Pessot, G. Mourou, IEEE J. Quantum Elecrton. 24 (1988) 398.
[26] H.R. Lange, A. Chiron, J.-F. Ripoche, A. Mysyrowicz, P. Breger, P. Agostini, Phys. Rev. Lett. 81 (1998) 1611.
[27] S. Tzortzakis, M.F. Franco, Y.-B. André, A. Chiron, B. Lamouroux, B.S. Prade, A. Mysyrowicz, Phys. Rev. E 60 (1999) 3505.
[28] H.D. Ladouceur, A.P. Baronavski, D. Lorhmann, P.W. Grounds, P.G. Girardi, Opt. Commun. 189 (2001) 107.
[29] S.L. Chin, A. Talebpour, J. Yang, S. Petit, V.P. Kandidov, O.G. Kosareva, M.P. Tamarov, Appl. Phys. B 74 (2002) 67.
[30] G. Méchain, A. Couairon, M. Franco, B. Prade, A. Mysyrowicz, Phys. Rev. Lett. 93 (2004) 035003.
[31] J. Kasparian, R. Sauerbrey, D. Mondelain, S. Niedermeier, J. Yu, J.-P. Wolf, Y.-B. André, M. Franco, B. Prade, S. Tzortzakis, A. Mysyrowicz, M. Rodriguez, H. Wille, L. Wöste, Opt. Lett. 25 (2000) 1397.
[32] V.P. Kandidov, O.G. Kosareva, A.A. Koltun, Quantum Electron. 33 (2003) 69.
[33] G. Fibich, G.C. Papanicolaou, Opt. Lett. 22 (1997) 1379.